CMS-PAS: SMP-14-011

Search for Electroweak-induced Production of Wγ with Two Jets and Anomalous Quartic Gauge Couplings in pp Collisions at $\sqrt{s} = 8$ TeV

中国物理学会高能物理分会第十二届全国粒子物理学术会议

杨大能　北京大学物理学院高能物理实验组

August 25th, 2016
USTC, Hefei

Outline

- Motivations
- Physics objects reconstruction and selection
- Background modelling
- Systematic uncertainties
- Search for EWK Wγ+jets signal
- Wγ+2jets cross section measurement
- Limits on anomalous couplings
- Summary

Motivations

Electroweak physics at the LHC

- Multi-boson production measurements help us confirm the gauge symmetry and understand better gauge-boson self-interactions
- Backgrounds of new physics search and decay products of BSM particles

***"Underlying structures"* of vector boson scattering events**

- Two forward quark jets with large Rapidity gap
- Color coherence
- Vector bosons within the rapidity gap

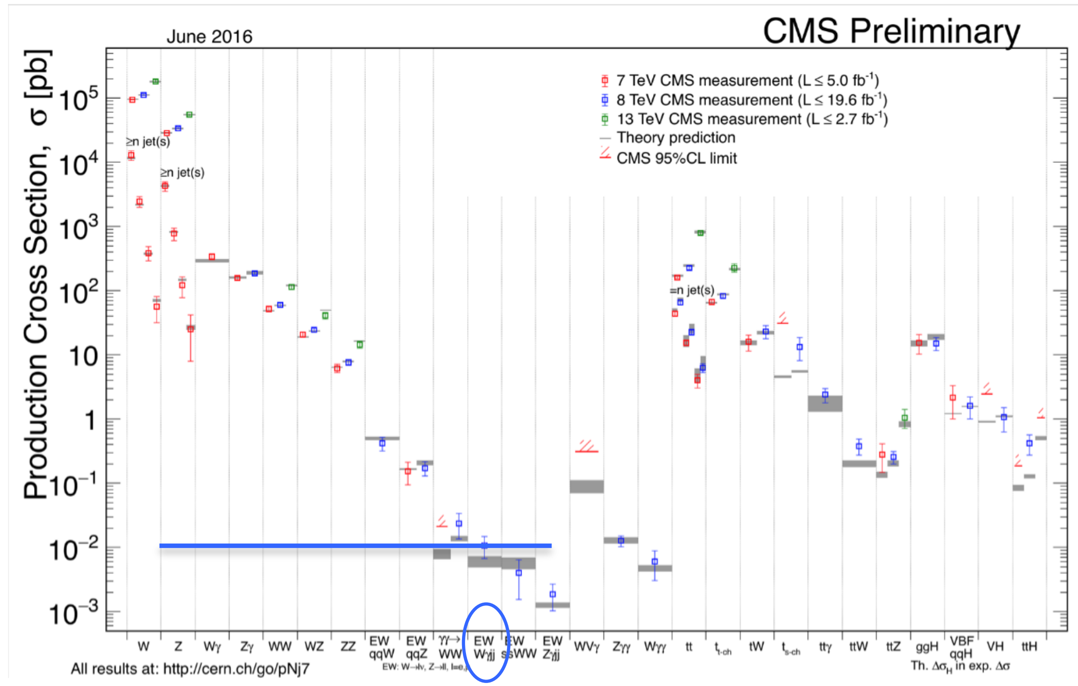

CMS-PAS: SMP-14-011

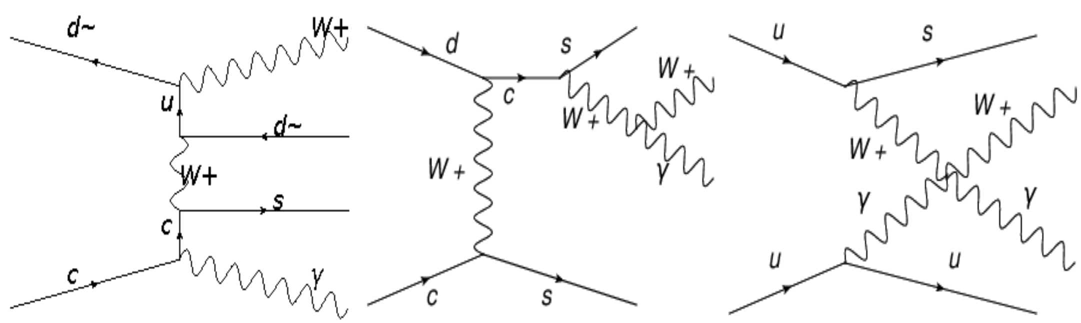

Event reconstruction

The Particle Flow algorithm

- Attempt to reconstruct all stable particles in an event
- Information from sub-detectors is combined in best possible way
- List of particles is returned

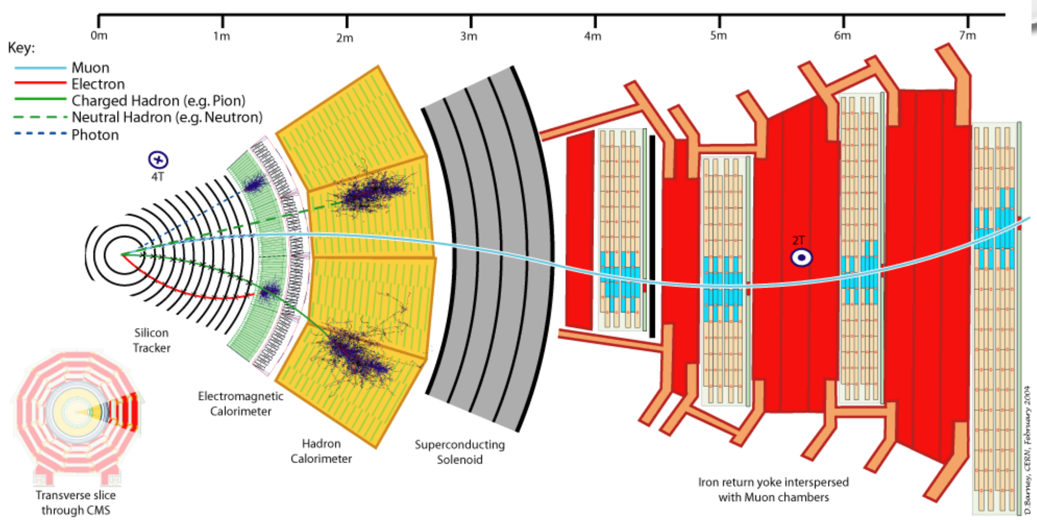

Primary vertex

- The one with at least 4 associated tracks and the sum of their p_T^2 is highest
- $|z| \leq 24cm, \rho \leq 2cm$

Muon

- ID efficiency 80%, veto ID efficiency 90%
- Particle flow based relative isolation

Electron

- Cut based ID. ID eff. 80%, veto ID eff. 90%
- Particle flow based relative isolation with EA correction

Missing Transverse Energy

- Energy scale correction

Photons

- Cut based shower shape and isolation ID
- Particle flow isolation

Jets

- Anti-k_T Particle flow jets with $\Delta R = 0.5$
- Charged Hadron not from PV removed
- Jet Energy Correction

Event selection

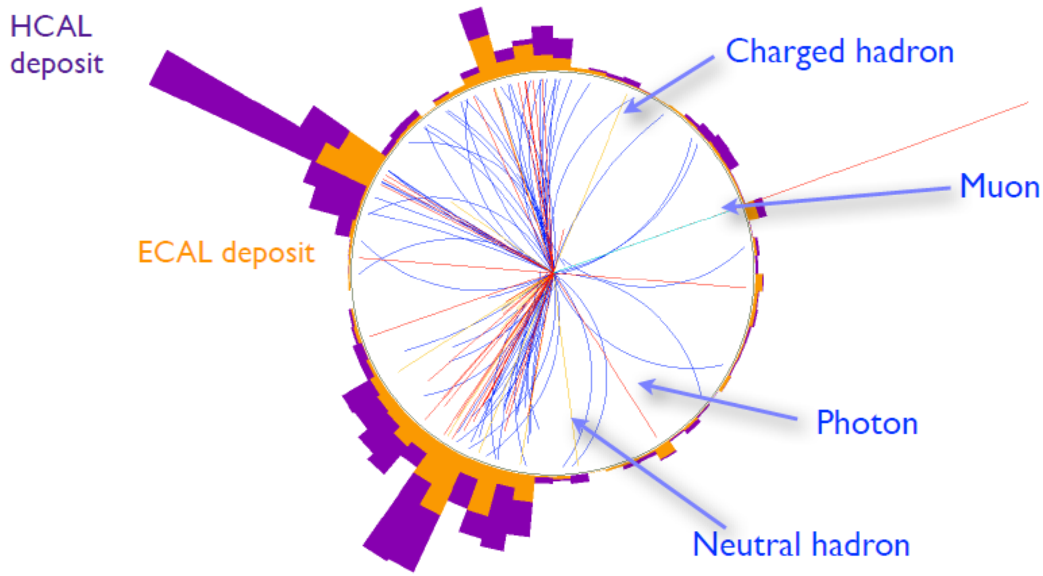

Figure from Florian Beaudette's (LLR) talk

Signal region only

- $|y_{W\gamma} - (y_{j1} + y_{j2})/2.0| < 0.6$,
- $|\Delta\phi_{W\gamma,dijet}| > 2.6$,
- $M_{jj} > 700$ GeV,
- $|\Delta\eta(j1, j2)| > 2.4$.

Base-line selections

Single lepton trigger	$p_T^{j1} > 40$, $p_T^{j2} > 30$ GeV
Lepton, photon ID and isolation	$\lvert\eta^{j1}\rvert < 4.7$, $\lvert\eta^{j2}\rvert < 4.7$
Second lepton veto	$\lvert\Delta\phi_{j1,\not{E}_T}\rvert > 0.4$, $\lvert\Delta\phi_{j2,\not{E}_T}\rvert > 0.4$
Muon (electron) $p_T > 25(30)$ GeV, $\lvert\eta\rvert < 2.1(2.4)$	B quark jet veto for tag jets
W transverse mass > 30 GeV	Dijet pair invariant mass $M_{jj} > 200$ GeV
$\not{E}_T > 35$ GeV	Photon $p_{T,\gamma} > 22$ GeV, $\lvert\eta\rvert < 1.44$
$\lvert M_{e\gamma} - M_Z\rvert > 10$ GeV (electron channel)	ΔR_{jj}, $\Delta R_{j\gamma}$, ΔR_{jl}, $\Delta R_{l\gamma} > 0.5$

Background modelling

Electron mis-identification background can be suppressed by using the selection $|M_{\gamma e} - M_Z| > 10$ GeV
Electron channel only

Ordered with decreasing size of the backgrounds

Using data to reduce the large theoretical uncertainty in the normalization of **QCD Wγ+jets** background

W+jets/multijets with one jet being mis-identified

γ+jets with one jet being mis-identified as an electron

- W+jets/multijets with one jet fakes a photon
- γ+jets with one jet fakes an electron
- QCD Wγ+jets normalization determined in a Mjj control region with 200 GeV < Mjj < 400 GeV

Other processes are taken from simulation, e.g. dibosons, single top, ttbar

Base-line selections are considered to ensure the quality of final state objects.

Estimation of photon contamination background

- **Photon contamination rate**
  - ✓ **Template sample used for the calculation**
  - ✓ ***Fake photon fraction***

$$(FF) = \frac{D(QCD\ only)}{D}$$

- **Normalizing a photon like jet sample according to the fake FF**
  - ✓ ***Scale factor*** $(p_T^{\gamma}) =$

$$FF * \frac{D}{PLJ\ events} = \frac{D(QCD\ only)}{PLJ\ events}$$

The normalized photon like jet sample provides photon contamination background for any kinematic distributions.

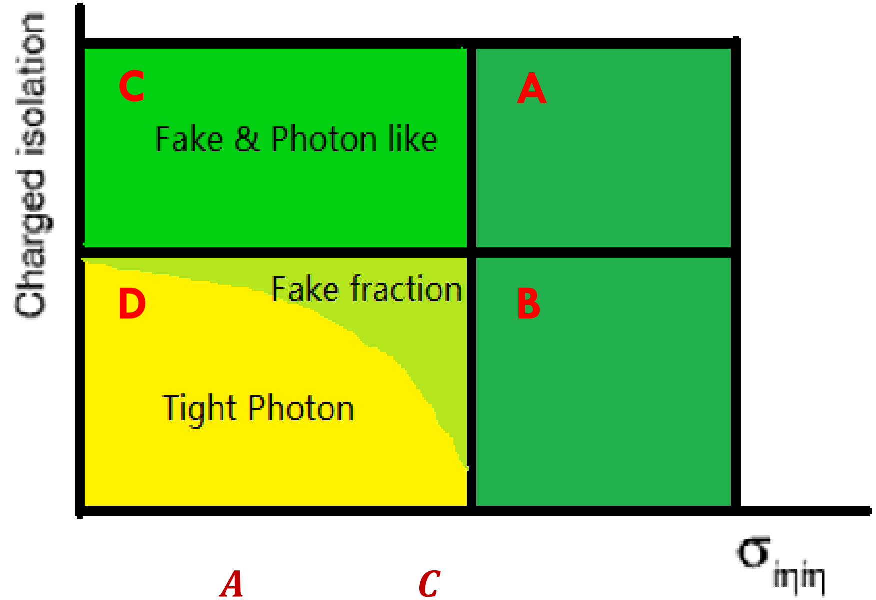

$$\frac{A}{B} = \frac{C}{D(QCD\ only)}$$

Uncertainty estimation

- Systematic uncertainty from charged isolation sideband and shower shape.
- From 13% at p_T^{γ}~25 GeV to 54% at p_T^{γ}> 135 GeV

γ+jets to electron contamination and QCD $W\gamma$+jets backgrounds

γ+jets to electron contamination

- The shape of missing transverse energy is used to extract the electron **contamination rate**. A data-based sample is normalized according to this rate. Similar as the estimation of photon contamination.

- The contribution of this background is negligible in the signal region but is important for QCD Wγ+jets estimation in the Mjj control region.

QCD Wγ+jets Mjj control region

- 200 GeV < Mjj < 400 GeV
- Base line selections

Muon channel

normalization scale factor: 0.772 ± 0.048

Electron channel

normalization scale factor: 0.773 ± 0.055

Theory K-factor from VBFNLO: 0.93 ± 0.27

Electron contamination background uncertainty

- Statistical uncertainty:16.7%
- Systematical uncertainty: 5.2%

QCD Wγ+jets uncertainty

- Normalization uncertainty 6.2%(muon) / 7.1%(electron)
- Systematic uncertainty on the extrapolation from low Mjj to high Mjj

Other systematic uncertainties

- **Theoretical uncertainty**
  PDF unc. CTEQ 61, 1 central + 20 pairs; 2.8%.
  Scale unc. Obtained by varying the central scale with a factor of 0.5 or 2, the closure results in a 20% uncertainty.

- **Jet energy scale and Jet energy resolution uncertainties**
  Jet p_T from simulation smeared to describe the data
  Propagated to Mjj shape

- **Luminosity 2.6%**

- **Generator level cuts 1%**

- **PU Modeling 1%**

- **Jet anti-b tag uncertainty**
  Scale factor 96.6% for combined secondary vetex algorism, with 2% uncertainty.
  This uncertainty is propagated to the signal region and leads to 8.3% uncertainty for the $t\bar{t}\gamma$ process and 22.6% uncertainty for the single top process.
  The effects on other processes are negligible.

- **Photon energy scale 1%**

- **Trigger 1%**

- **Lepton RECO/ID efficiency Scale factor 2%**

Data and MC Comparison

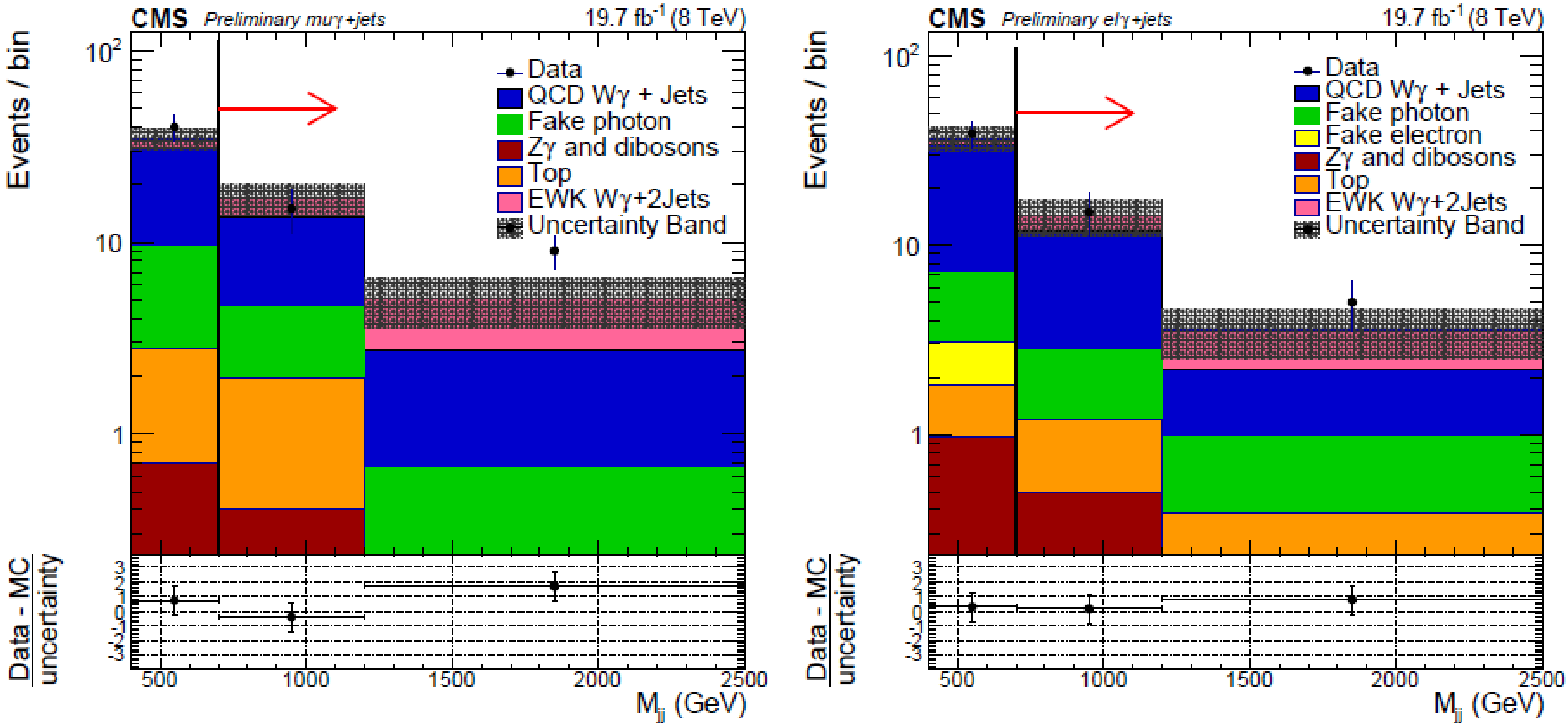

Comparison between predicted and observed Mjj distribution in **muon** **(left)** and **electron** **(right)** channels

The uncertainty band combines both statistical uncertainty and systematical uncertainties

Search for EWK Wγ+jets signal

Upper limit on the signal strength

- Using binned Mjij shape for limit calculation
- Full CLs construction

☐ CMS-NOTE-2011-005 (2011)

Process	Muon channel	Electron channel
EWK-induced Wγ+2jets	5.8 ± 1.8	3.8 ± 1.2
QCD-induced Wγ+jets	11.2 ± 3.2	10.3 ± 3.2
W + jets, 1 jet $\rightarrow \gamma$	3.1 ± 0.8	2.2 ± 0.6
MC $t\bar{t}\gamma$	1.2 ± 0.6	0.4 ± 0.2
MC single top quark	0.5 ± 0.5	0.6 ± 0.4
MC WVγ, V$\rightarrow$ two jets	0.3 ± 0.2	0.3 ± 0.2
MC Zγ + jets	0.2 ± 0.2	0.3 ± 0.2
Total prediction	22.1 ± 3.8	17.9 ± 3.5
Data	24	20

-- Expected significance –
1.5 σ
-- Observed significance –
2.7 σ

Observed limit (95% CL.)	4.3
Expected limit (median)	2.0
Expected limit (1σ)	3.5
Expected limit (2σ)	6.1

-- Best fit signal strength –
$\hat{\mu} = 1.78^{+0.99}_{-0.76}$ (68% CL.)

Wγ+2jets cross section measurement

From signal strength to cross sections:

$$\sigma_{fiducial\ region} = \sigma_{generator} \cdot \hat{\mu} \cdot \epsilon_{generated\ to\ fiducial}$$

A 4.8% interference effect is not included as uncertainty, since there is a large correlation with the scale uncertainty.

The normalization of QCD signal is changed to use NLO/LO correction factor.

Fiducial region definition

- $p_T^{j1} > 30$ GeV, $|\eta^{j1}| < 4.7$,
- $p_T^{j2} > 30$ GeV, $|\eta^{j2}| < 4.7$,
- $M_{jj} > 700$ GeV, $|\Delta\eta(j,j)| > 2.4$,
- $p_T^{l} > 20$ GeV, $|\eta^{l}| < 2.4$,
- $p_T^{\gamma} > 20$ GeV, $|\eta^{\gamma}| < 1.4442$,
- $\not{E}_T > 20$ GeV,
- $\Delta R_{j,j}, \Delta R_{l,j}, \Delta R_{\gamma,j}, \Delta R_{l,\gamma} > 0.4$.

Items	EWK measurement	EWK+QCD measurement
$\hat{\mu}$	$1.78^{+0.99}_{-0.76}$	$0.99^{+0.21}_{-0.19}$
EWK fraction (search region)	100%	27.1%
EWK fraction (fiducial region)	100%	25.8%
Observed (Expected) significance	2.67(1.52) σ	7.69(7.49) σ
Theory cross section (fb)	6.1 ± 1.2 (scale) ± 0.2 (PDF)	23.5 ± 6.6 (scale) ± 0.8 (PDF)
Measured cross section (fb)	10.8 ± 4.1 (stat.) ± 3.4 (syst.) ± 0.3 (lumi.)	23.2 ± 4.3 (stat.) ± 1.7 (syst.) ± 0.6 (lumi.)

Good agreement with theory predictions.

The ΔNLL limits

We consider an effective field theory with SU(2)⊗U(1) gauge symmetry linearly realized and with higher dimensional operators containing pure quartic couplings.
Reference: arXiv:hep-ph/0606118

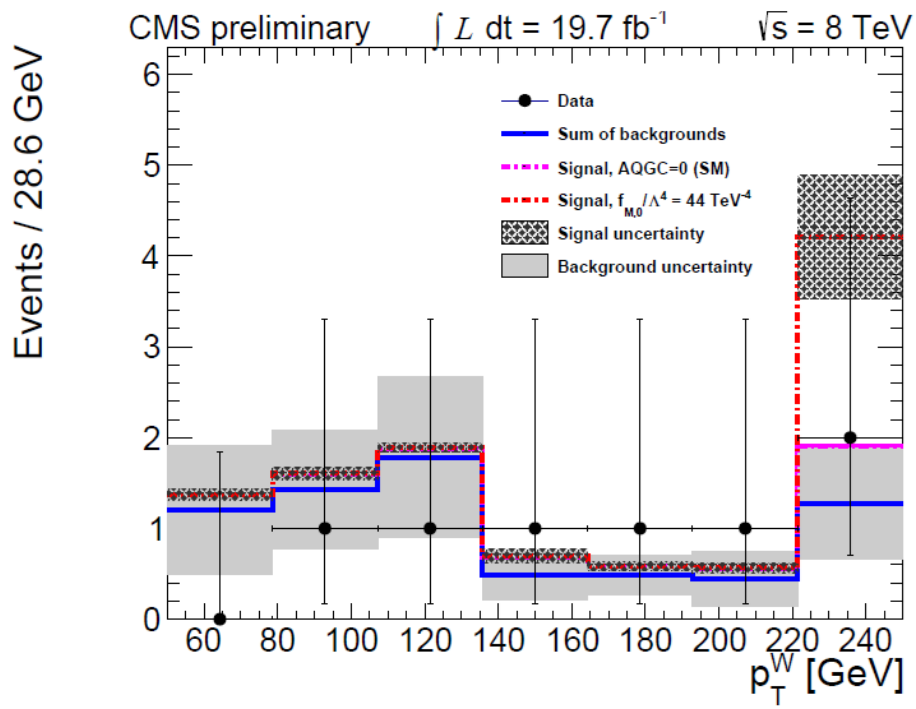

Comparison of predicted and observed distributions with electron and muon combined channels. The last p_T^W bin has been extended to include overflow contribution.

A change of selections for the aQGC study

- p_T^γ **> 200 GeV**
- $|y_{W\gamma} - \frac{y_{j1}+y_{j2}}{2}|$ <1.2, $|\Delta\eta_{jj}|$>2.4

Likelihood based statistical study

$$t_{\alpha_{test}} = -2ln\frac{\mathcal{L}(\alpha_{test},\hat{\hat{\theta}})}{\mathcal{L}(\hat{\alpha},\hat{\theta})},$$

t = -2*ΔNLL;
ΔNLL = L(minimize(ϑ)) – L(best fit)

$$\mathcal{L}(A,\theta) = norm(\theta) \cdot Poisson(N|\ S+B) \prod_n^N P(p^n_{T,W}, A)$$

Comparison with existing limits

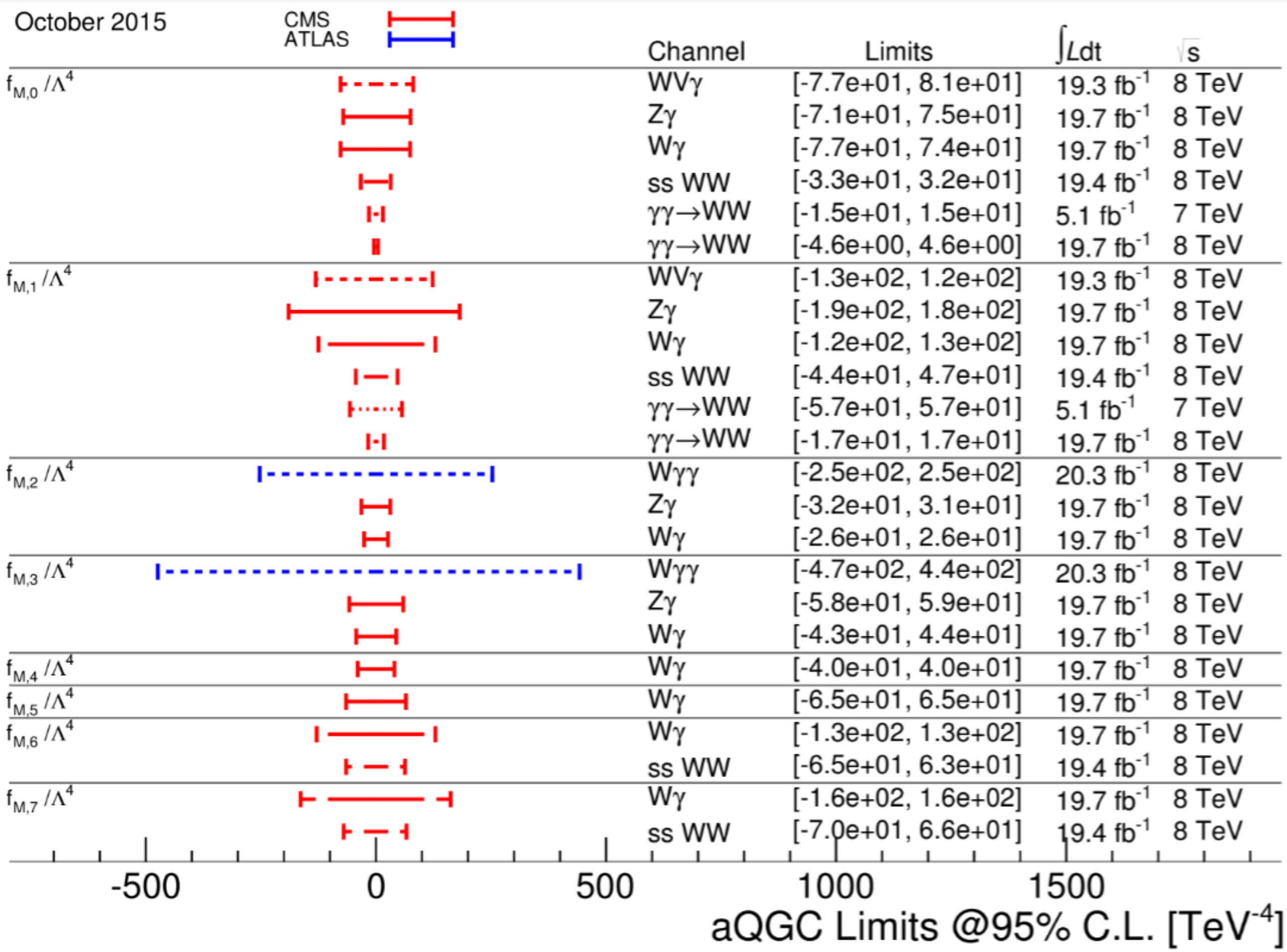

WVγ CMS: Phys. Rev. D **90** (2014) 032008
same sign WW: Phys. Rev. Lett **114** (2014) no. 5, 051801
VBS Zγ: CMS-PAS-SMP-14-018
Exclusive $\gamma\gamma \to WW$ CMS: JHEP **07** (2013) 116
W$\gamma\gamma$ ATLAS: Phys. Rev. Lett. **115** (2015), no. 3, 031802

Comparison with existing limits

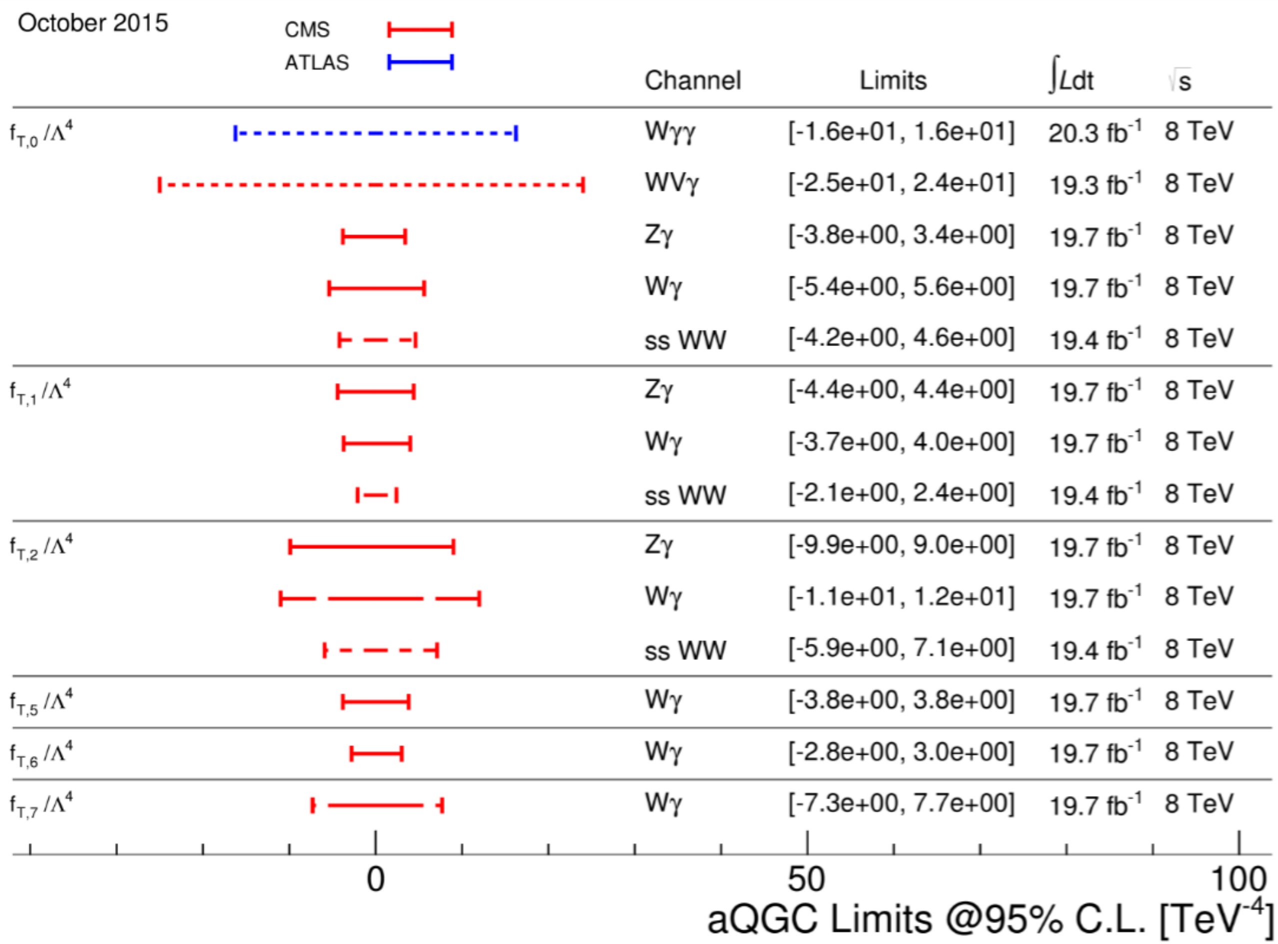

$WV\gamma$ CMS: Phys. Rev. D **90** (2014) 032008
same sign WW: Phys. Rev. Lett **114** (2014) no. 5, 051801
VBS $Z\gamma$: CMS-PAS-SMP-14-018
Exclusive $\gamma\gamma \rightarrow WW$ CMS: JHEP **07** (2013) 116
$W\gamma\gamma$ ATLAS: Phys. Rev. Lett. **115** (2015), no. 3, 031802

Summary

- Significance wrt no EWK signal is found to be 2.7 σ, the cross section in the fiducial region is measured to be 10.8 $\pm$ 4.1 (stat.) $\pm$ 3.4 (syst.) $\pm$ 0.3 (lumi.) fb, being consistent with the standard model predictions.

- The cross section measured with only non-Wγ plus two jets contribution as background is 23.2 $\pm$ 4.3 (stat.) $\pm$ 1.7 (syst.) $\pm$ 0.6 (lumi.) fb, which is consistent with the SM EWK+QCD prediction.

- Experimental limits on dimension eight anomalous quartic gauge couplings $f_{M,0-7}/\Lambda^4$, $f_{T,0-2}/\Lambda^4$, and $f_{T,5-7}/\Lambda^4$ are set at 95% confidence level.

- We will be able to measure the process more precisely using the 13 TeV data.

BACKUP

The ΔNLL limits

Observed Limits	Expected Limits
-77 (TeV^{-4}) $< f_{M0}/\Lambda^4 <$ 74 (TeV^{-4})	-47 (TeV^{-4}) $< f_{M0}/\Lambda^4 <$ 44 (TeV^{-4})
-125 (TeV^{-4}) $< f_{M1}/\Lambda^4 <$ 129 (TeV^{-4})	-72 (TeV^{-4}) $< f_{M1}/\Lambda^4 <$ 79 (TeV^{-4})
-26 (TeV^{-4}) $< f_{M2}/\Lambda^4 <$ 26 (TeV^{-4})	-16 (TeV^{-4}) $< f_{M2}/\Lambda^4 <$ 15 (TeV^{-4})
-43 (TeV^{-4}) $< f_{M3}/\Lambda^4 <$ 44 (TeV^{-4})	-25 (TeV^{-4}) $< f_{M3}/\Lambda^4 <$ 27 (TeV^{-4})
-40 (TeV^{-4}) $< f_{M4}/\Lambda^4 <$ 40 (TeV^{-4})	-23 (TeV^{-4}) $< f_{M4}/\Lambda^4 <$ 24 (TeV^{-4})
-65 (TeV^{-4}) $< f_{M5}/\Lambda^4 <$ 65 (TeV^{-4})	-39 (TeV^{-4}) $< f_{M5}/\Lambda^4 <$ 39 (TeV^{-4})
-129 (TeV^{-4}) $< f_{M6}/\Lambda^4 <$ 129 (TeV^{-4})	-77 (TeV^{-4}) $< f_{M6}/\Lambda^4 <$ 77 (TeV^{-4})
-164 (TeV^{-4}) $< f_{M7}/\Lambda^4 <$ 162 (TeV^{-4})	-99 (TeV^{-4}) $< f_{M7}/\Lambda^4 <$ 97 (TeV^{-4})
-5.4 (TeV^{-4}) $< f_{T0}/\Lambda^4 <$ 5.6 (TeV^{-4})	-3.2 (TeV^{-4}) $< f_{T0}/\Lambda^4 <$ 3.4 (TeV^{-4})
-3.7 (TeV^{-4}) $< f_{T1}/\Lambda^4 <$ 4.0 (TeV^{-4})	-2.2 (TeV^{-4}) $< f_{T1}/\Lambda^4 <$ 2.5 (TeV^{-4})
-11 (TeV^{-4}) $< f_{T2}/\Lambda^4 <$ 12 (TeV^{-4})	-6.3 (TeV^{-4}) $< f_{T2}/\Lambda^4 <$ 7.9 (TeV^{-4})
-3.8 (TeV^{-4}) $< f_{T5}/\Lambda^4 <$ 3.8 (TeV^{-4})	-2.3 (TeV^{-4}) $< f_{T5}/\Lambda^4 <$ 2.4 (TeV^{-4})
-2.8 (TeV^{-4}) $< f_{T6}/\Lambda^4 <$ 3.0 (TeV^{-4})	-1.7 (TeV^{-4}) $< f_{T6}/\Lambda^4 <$ 1.9 (TeV^{-4})
-7.3 (TeV^{-4}) $< f_{T7}/\Lambda^4 <$ 7.7 (TeV^{-4})	-4.4 (TeV^{-4}) $< f_{T7}/\Lambda^4 <$ 4.7 (TeV^{-4})

Theoretical framework

Symmetries and Particle content

- Effective field theory with SU(2)⊗U(1) gauge symmetry implemented for high order operators

- Linear realization of the gauge symmetry implements the "pure" quartic couplings with dimension 8 and higher dimension operators

- Reference: arXiv:hep-ph/0606118, different convention with the VBFNLO

$$
\begin{aligned}
f_{S,0,1} &= f^{\text{Éboli}}_{S,0,1} \\
f_{M,0,1} &= -\frac{1}{g^2} \cdot f^{\text{Éboli}}_{M,0,1} \\
f_{M,2,3} &= -\frac{4}{g'^2} \cdot f^{\text{Éboli}}_{M,2,3} \\
f_{M,4,5} &= -\frac{2}{gg'} \cdot f^{\text{Éboli}}_{M,4,5} \\
f_{M,6,7} &= -\frac{1}{g^2} \cdot f^{\text{Éboli}}_{M,6,7} \\
f_{T,0,1,2} &= \frac{1}{g^4} \cdot f^{\text{Éboli}}_{T,0,1,2} \\
f_{T,5,6,7} &= \frac{4}{g^2 g'^2} \cdot f^{\text{Éboli}}_{T,5,6,7} \\
f_{T,8,9} &= \frac{16}{g'^4} \cdot f^{\text{Éboli}}_{T,8,9}
\end{aligned}
$$

The LM5 operator in the reference is not hermitian, we have got confirmation from the authors. We also thank Mr. X. Wang, Y. Zhang for helping with the cross check.